MULTI-OUTPUT REGRESSION PREDICTION OF PNEUMATIC SUBMERGING RESISTANCE AND DISTURBANCE AREA BASED ON NEURAL NETWORK
/
基于神经网络的气动深松阻力及扰动面积多输出回归预测

Xia LI[1,2], Xuhui WANG[1,2], Jinyou XU*[1,2], Xinglong LI [1,2], Zhangjun JIANG[1,2], Birong YOU[1,2]
[1)] Tianjin Key Laboratory for Advanced Mechatronic System Design and Intelligent Control, School of Mechanical Engineering, Tianjin University of Technology, Tianjin / China;
[2)] National Demonstration Center for Experimental Mechanical and Electrical Engineering Education, Tianjin University of Technology, Tianjin / China
Tel: +15200158817; E-mail: yj20220152@stud.tjut.edu.cn
DOI: https://doi.org/10.35633/inmateh-73-47

Keywords: *pneumatic subsoiling, neural network, multiple output regression prediction, traction resistance, disturbed area*

ABSTRACT
The current field of pneumatic subsoiling prediction focuses on a single task and neglects the possible interrelationships between different outputs. In order to improve prediction accuracy and reduce the number of algorithmic model establishments, this study conducted field experiments on soil in autumn and winter. Neural network algorithms RBF (radial basis neural network), BP (backward propagation neural network), DNN (deep learning network), and CNN (convolutional neural network) were used to make multi-output regression predictions for changing the traction resistance and disturbance area affected by different levels of subsoiling velocity, depth, and pressure value in the process of pneumatic subsoiling. The evaluation indexes RMSE, MAE, and R^2 were compared with the single output regression model, and the accuracy of the four models with the highest accuracy was compared with that of its own single output model to prove the correlation between traction resistance and disturbance area. The results showed that the R^2 of the four model test sets of RBF, BP, DNN, and CNN were 0.9999, 0.9966, 0.9986, and 0.9762, respectively. The R^2 values of the disturbance area are 0.9997, 0.9924, 0.9968, and 0.9715, respectively. RBF has the highest R2 and the lowest RMSE and MAE, indicating that the RBF model has the best prediction effect. Compared with the single output regression model of the RBF model, the prediction accuracy of both outputs is higher, so it can be used to predict the subsoiling drag resistance and disturbance area.

摘要
针对目前气动深松预测领域多聚焦于单一任务，忽略了不同输出之间可能存在的相互关系。为了提高预测的精确性，并且减少算法模型建立次数，本研究对秋冬两个季节下的土壤进行田间试验，利用神经网络算法 RBF（径向基神经网络）、BP（逆向传播神经网络）、DNN（深度学习网络）、CNN（卷积神经网络）对气动深松过程中改变受不同水平的深松速度、深度、气压值影响的牵引阻力及扰动面积值进行多输出回归预测，利用评价指标 RMSE、MAE、R^2 与单输出回归模型进行对比评估，将四个模型中精度最高的与本身的单输出模型的精度进行对比，证明牵引阻力及扰动面积之间的相关性。结果表明：RBF、BP、DNN、CNN 四个模型测试集牵引阻力的 R^2 分别为 0.9999、0.9966、0.9986、0.9762。扰动面积的 R^2 分别为 0.9997、0.9924、0.9968、0.9715。RBF 的 R^2 最高，RMSE、MAE 最低，可见 RBF 模型预测效果效果最好，且相较于 RBF 模型的单输出回归模型两个输出的预测精度都较高，因此可用于深松牵引阻力及扰动面积的预测。

INTRODUCTION
Soil is the basis of sustainable agricultural development (*Lou et al., 2021*). Compaction is one of the factors causing soil degradation (*Iman et al., 2017*), which makes the soil more vulnerable to erosion by wind and water, causing economic and ecological damage to society (*Thomas et al., 2019*). It is urgent to improve compaction and break the bottom of the plow (*Su et al., 2021*).

Xia Li, Ph.D. Eng.; Xuhui Wang, MS.Stud.Eng.; Jinyou Xu, Associate Prof, Ph.D. Eng.; Xinglong Li, MS.Stud.Eng.; Zhangjun Jiang, MS.Stud.Eng.; Birong You, MS.Stud.Eng.

A subsoiler is a mechanical device that acts on soil (*Odey et al., 2018*), which can crush soil, increase soil moisture content, and promote plant root growth (*Aday et al., 2019*). Plowing in compacted soil requires high traction (*Askari et al., 2017*). Many ways of reducing drag have been studied at home and abroad, such as vibration and pneumatic drag reduction. Different drag reduction methods have their own characteristics.

Vibration subsoiling relies on vibration to reduce drag. Shi et al. explored the disturbance effect of vibration subsoiling on soil by using the discrete element method combined with field test verification (*Shi. et al., 2021*). By using the TST5910 dynamic signal test and analysis system, Dong et al. tested and analyzed the vibration response characteristics of the frame of the 1ST-460 vibration subsoiler (*Dong et al., 2022*).

Compared with vibration subsoiling, pneumatic subsoiling uses high-pressure gas to break through the soil aggregates at the bottom of the plough, thus reducing the resistance and strengthening the soil disturbance. Zuo et al. used pneumatic subsoiling to conduct air jet tests on cultivated soil, analyzed the characteristics of pneumatic subsoiling, and verified the feasibility of pneumatic subsoiling (*Zuo et al., 2016; Zuo et al., 2017*). Zhang designed a hot-air subsoiling machine and explored the subsoiling characteristics of the hot-air subsoiling machine combined with the soil tank test (*Zhang et al., 2022*). Feng et al. conducted a simulation test of pneumatic subsoiling based on the pressure splitting method and explored the effect of pneumatic subsoiling operation under the combination test of different pressure values and subsoiling depth (*Feng. et al., 2019*). Li et al. established an aerodynamic model of pneumatic subsoiling and explored the effects of three factors, namely different plowing depth, air pressure, and speed, on traction resistance (*Li et al., 2022*). Su et al. investigated the vibration characteristics of the pneumatic subsoiler and optimized the structure of the subsoiler. The optimized subsoiler avoids resonance phenomena and prolongs service life (*Su. et al., 2022*). Zuo et al. explored the variation rule of soil porosity in pneumatic deep panasonic and analyzed the porosity increase rate as an index. The results show that the atmospheric pressure and horizontal distance have a significant effect on the porosity increase rate (*Zuo et al., 2017*).

The application of machine learning to agriculture can help researchers save a lot of time and experience. In order to reduce the maintenance cost of machine damage caused by abnormal operation, *Gao et al.* (*2022*) realized the control of tillage under the condition of non-uniform soil height in the field. Improved random forest was used to conduct regression prediction of tillage depth, and a prediction model of tillage depth was established.

Li et al. (2023) used RF, SVR, XGBoost and BP models to make regression prediction of traction resistance in the process of pneumatic subsoiling by taking five factors as input: ploughing depth, velocity, air pressure, soil bulk density and water content. The results showed that the prediction accuracy of RF model was the highest (*Li et al., 2023*). When the output of the regression prediction is multiple dimensions, the number of models required will be reduced, and the prediction accuracy of the model can also be improved if there is a correlation between the multiple output factors. In order to optimize the pneumatic subsoiler, it is very important to explore the relationship between the pneumatic subsoiler and soil parameters. It is of great significance to apply multi-output neural network model to pneumatic subsoiling.

In this study, four neural network models, RBF, BP, DNN, and CNN, were used to simultaneously predict the traction resistance and soil disturbance area in different seasons at the same location on the basis of pneumatic subsoiling. Then, the model with the highest prediction accuracy was found among the four models. When comparing the single prediction of the traction resistance and disturbance area of the model, the accuracy of the model was improved.

MATERIALS AND METHODS

Test site and materials

The test site is located in the experimental field (39°19'n, 116°17'e) outside Langfang Ward Technology Co., LTD., 40 meters northwest of the intersection of 602 Xiang Road and Huimin East Road, Liuquan Town, Gu'an County, Langfang City, Hebei Province. The soil type of the experimental field was loam (clay 12.1%; silica 39.8%; sand 48.1%). The tractor is a John Deere 6B-954 tractor. The test shovel is a chisel-type shovel with air holes at the tip of the crank shovel. The model is JBT9788-1999. There is also an S-type digital tension meter, a laptop, a plugboard, and an air pump. The air pump is connected with the subsoiling shovel through the gas pipe to realize pneumatic subsoiling.

The details are shown in Figure 1 below.

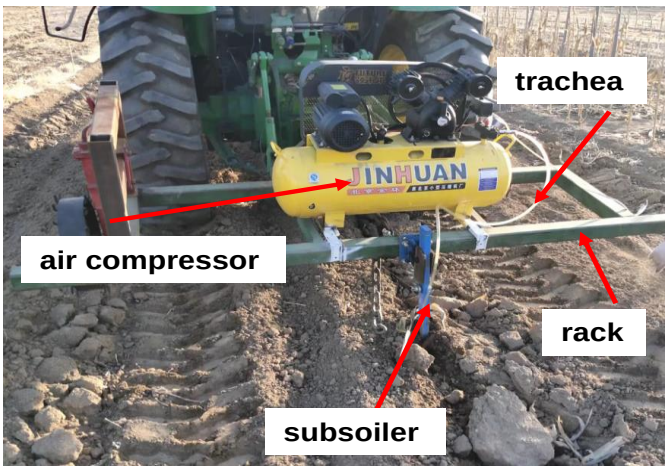

Fig.1 - Pneumatic subsoiling equipment

The experimental data include traction resistance and disturbance area, in which the traction resistance is obtained by the tension sensor. The tension sensor is connected by a chain to one end of the subsoiling shovel and the other end to the frame, which is powered by a battery. In the process of subsoiling, the subsoiling shovel pulls the iron chain to generate traction resistance, and the tension sensor receives the value and transmits it to the computer, as shown in Figure 2(a). The disturbance surface is obtained by the plugboard method, as shown in Figure 2(b) below. The insert board is composed of a wood strip with a length and width of 10 mm and a height of 500 mm, respectively. After the loose soil has been deeply loosened to reveal the disturbed surface, place the insert board on it. Then place A2 paper behind the insert board and trace the shape of the disturbed surface along the top of the strip.

(a) *(b)*

Fig. 2 - Traction resistance and disturbance area data acquisition

The data were divided into two groups, one in the autumn and one in the winter. In order to measure the moisture content and bulk density of soil in different seasons, 100 cm^3 soil samples were randomly sampled at 12 points in the field by the ring knife method. Taking the dry mass of the soil as the soil volume, the soil sample was placed in a drying oven with a temperature of 105° for 24 hours, and the soil bulk density was obtained after being weighed again. The soil water content was measured at 12 points, and the soil depth range of water content collection was 20-30 cm. The specific operation method is to weigh the collected soil once, then put it in the oven to dry until the water completely evaporates, and then weigh the dried soil. The proportion of the reduced value of the soil weight in the dried soil weight is the moisture content. The collected autumn and winter soil parameters are shown in the following table:

Table 1

Soil parameters in autumn and winter

Season	Moisture content (%)	Unit weight (kg/m^3)
Autumn	20.9	1580
Winter	18.3	1940

In the field experiment, there were 5 levels of working pressure (0, 0.2, 0.4, 0.6, 0.8 MPa), 3 levels of subsoiling speed (1, 2, 3), and 4 levels of subsoiling depth (20, 25, 30, 35 cm). Traction resistance and disturbance surface data were respectively measured in the experiments of the two seasons, with 60 sets of data for each season and a total of 120 sets of data. In Figures 3-4, the four tillage depths were taken as horizontal coordinates to compare the changes in traction resistance and disturbance area under different pressures and tillage speeds. It can be seen from the figure that the traction resistance in winter is significantly higher than that in autumn, and the disturbance area is smaller than that in autumn.

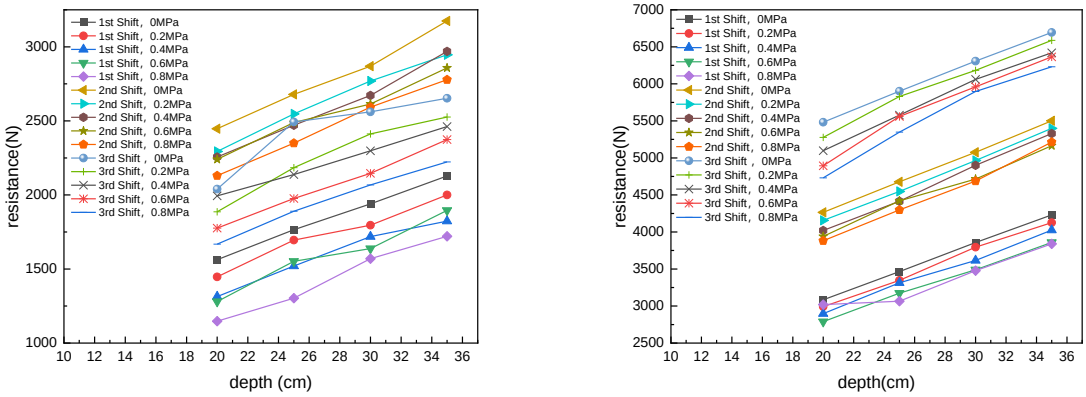

Autumn *Winter*

Fig. 3 - Traction resistance data at different velocities, depths, and working pressures

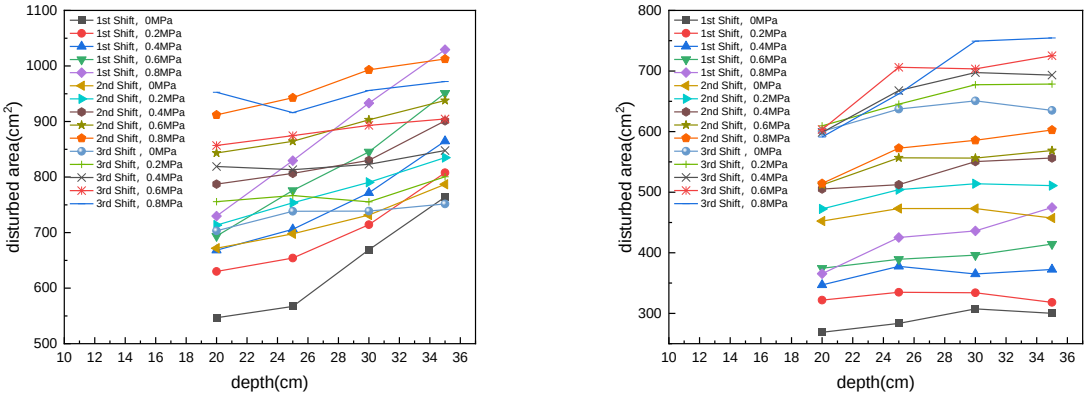

Autumn *Winter*

Fig. 4 - Disturbance area data at different velocities, depths, and working pressures

Neural network multiple output regression prediction model

RBF neural network: It is a radial basis neural network with an uncomplicated structure and three layers, namely the input layer, hidden layer, and output layer. Because of its simple structure, fast learning speed, and ability to approximate arbitrary nonlinear functions (*Kou, 2022*), it is often widely used in the fields of time series analysis, pattern recognition, graph processing, etc. The mathematical expression of the model refers to the formula in Melagraki's paper as follows (*Melagraki. et al., 2006*):

$$y_j = \sum_{i=1}^{n} \omega_{ij} e^{-\frac{\|x_p - c_i\|^2}{2\sigma^2}} \quad (j = 1, 2, \cdots, p) \tag{1}$$

Where: y_j is the jth output of the network;

ω_{ij} - the link weight from the hidden layer to the output layer;

n - the number of hidden layer nodes;

X_p - the Pth input sample;

c_i - the center of the network hidden layer node;

σ - the variance of the Gaussian function.

A BP neural network is a kind of neural network based on error-reverse propagation that contains only one hidden layer and can approximate any nonlinear system with arbitrary accuracy (*Wang, 2014*). The number of nodes in the hidden layer is calculated by referring to the following formula 2 in Qian's paper (*Qian. et al., 2021*). During the training process, the BP model constantly updates itself to fit the characteristics of new data. Therefore, the model has very high adaptability (*Tang, 2018*).

$$a \le 4\sqrt{i(y+3)+1} \tag{2}$$

where: a is the number of neurons in the hidden layer;

i - the number of neurons in the input layer;

y - the number of neurons in the output layer;

When the number of hidden layer neurons in the BP neural network used in this study is calculated to be 10, the prediction effect is the best.

DNN is a deep learning network with one input layer, multiple hidden layers, and one output layer, and the hidden layers are fully connected. There are four processes in training DNN models: forward propagation, reverse propagation, weight gradient calculation, and updating. The core of the forward propagation process is to calculate the next hidden layer from the previous hidden layer, and the specific equation is as follows: The focus of backpropagation is to use the gradient of loss function to calculate the gradient of weight and bias and use the chain rule to backpropagate the gradient layer by layer. The output formula 3 of the DNN model is shown as follows in Song's paper (*Song et al., 2019*):

$$y = f\left(\sum_{i=1}^{n} \omega_i x_i + \theta\right) \tag{3}$$

where: ω_i is the weight coefficient;

n - the number of neurons in the input layer;

X_i - the neural network input;

θ - the bias;

f is the activation function;

CNN Neural Network: The CNN network has been widely used in image recognition, object detection, and other fields, has achieved good results, and is also used to perform data regression prediction tasks. The structure of the neural network includes a convolutional layer, a pooling layer, and a fully connected layer.

RESULTS

Multiple output prediction results

In this experiment, five factors that can affect the effect of pneumatic subsoiling, namely subsoiling speed, depth, pressure value, moisture content, and soil bulk density, were selected as input indexes for model training, and the predicted results were traction resistance and disturbance area. The 60 groups of data from the autumn experiment and the 60 groups of data from the winter experiment were combined to build a data set, and the 120 groups of data were randomly arranged, with the first 60 groups of data used in the model training process and the last 10 groups of data used in the test process. When building the model, it is necessary to normalize the data, then train the model with the training set, verify the model with the test set after the training is completed, and then reverse normalize the predicted data and calculate the error to evaluate the model performance.

In this study, MATLAB 2023a software was used for modeling. Open the software to create four windows, and enter the code for each neural network. Figures 5-12 show the specific prediction results:

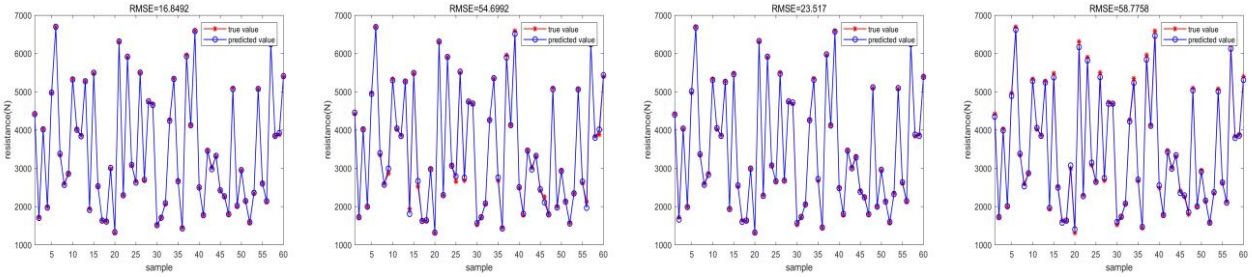

RBF *BP* *DNN* *CNN*

Fig. 5 - The fitting plot of four models when predicting traction resistance in the training set

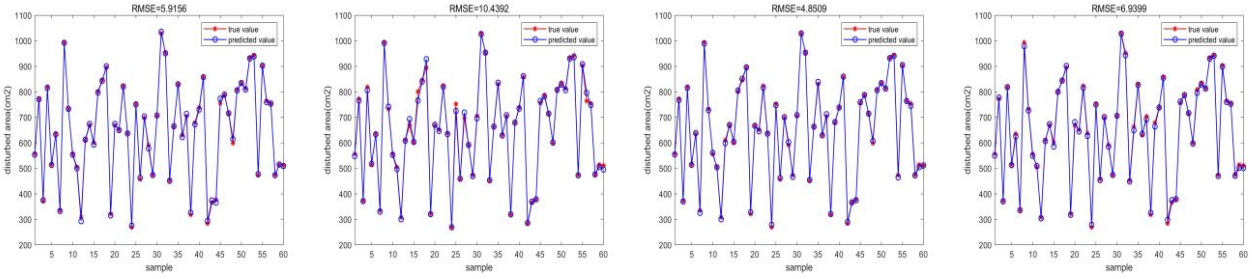

RBF *BP* *DNN* *CNN*

Fig. 6 - The fitting plot of four models when predicting the disturbance area in the training set

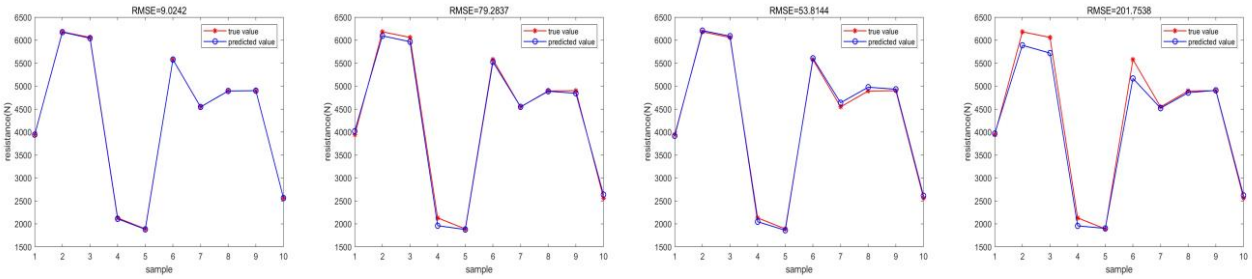

RBF *BP* *DNN* *CNN*

Fig. 7 - The fitting plot of the four models when predicting traction resistance in the test set

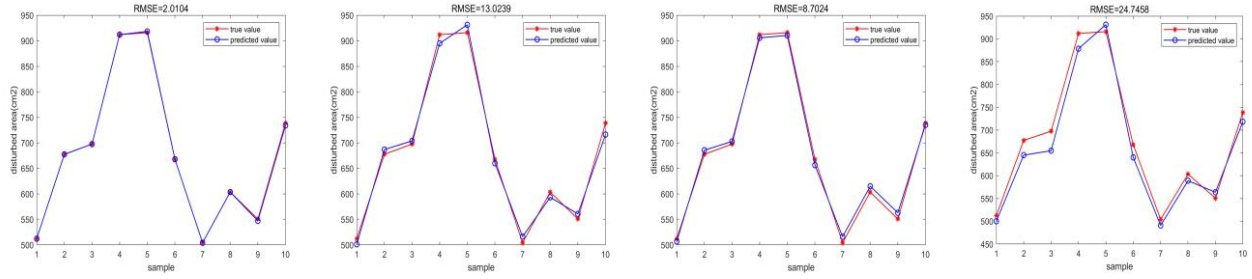

RBF *BP* *DNN* *CNN*

Fig. 8 - The fitting plot of the four models when predicting the disturbance area in the test set

The graph below is a regression graph of the four neural networks, representing the degree of fit of the respective models. The higher the degree of fitting, the smaller the error between the true value and the predicted value, and the better the prediction effect of the network.

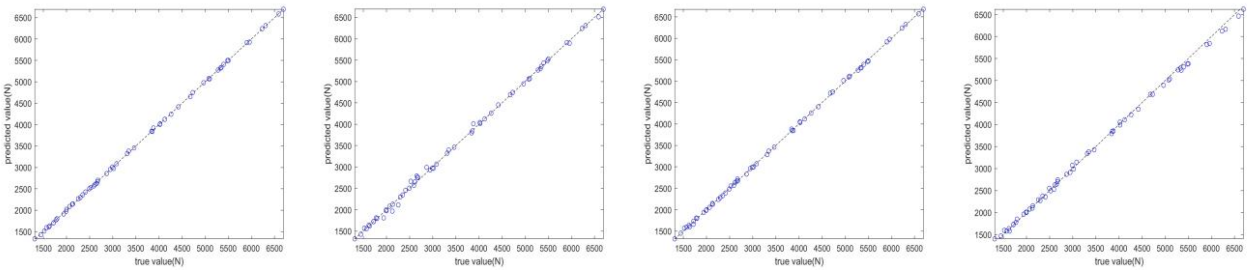

RBF *BP* *DNN* *CNN*

Fig. 9 - The regression plot of four models predicting traction resistance in the training set

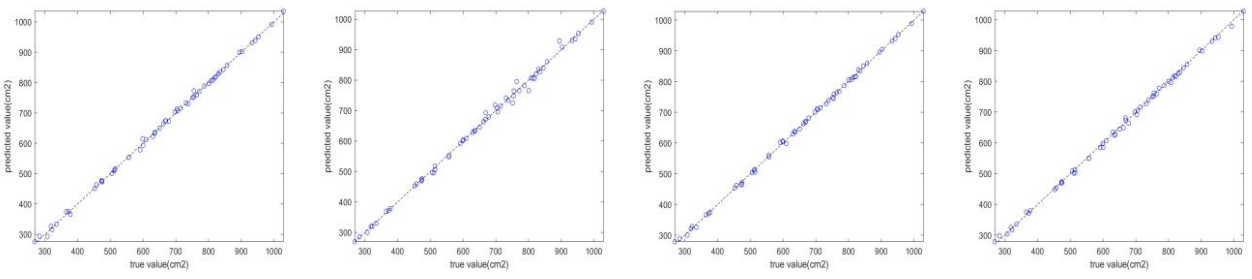

RBF *BP* *DNN* *CNN*

Fig. 10 - The regression plot of four models predicting the disturbance area in the training set

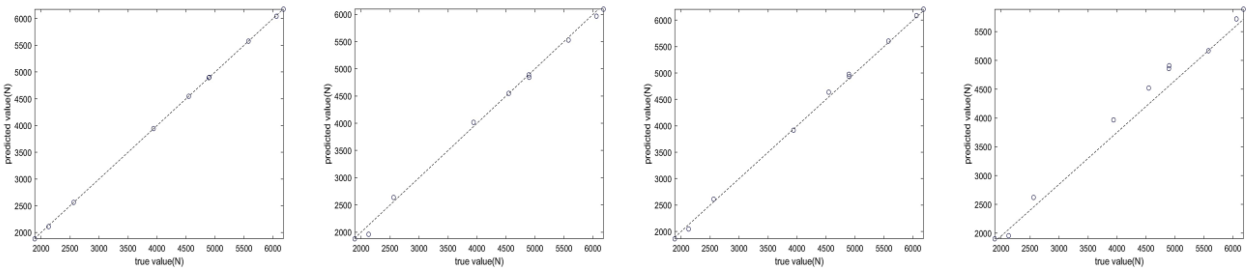

RBF *BP* *DNN* *CNN*

Fig. 11 - The regression plot of four models predicting traction resistance in the test set

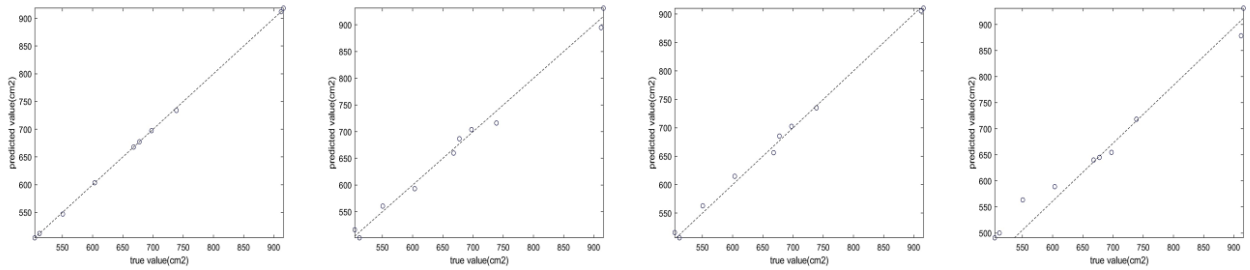

RBF *BP* *DNN* *CNN*

Fig. 12 - The regression plot of four models predicting the disturbance area in the test set

After the regression prediction calculation of the model, the measured results of the performance evaluation coefficients of the four models are shown in the table below and the radar chart. Through comparative analysis, it can be seen that among the four models in the prediction results, the prediction accuracy of the CNN model is the lowest, and the R^2 value of the prediction data of traction resistance and disturbance area of the RBF model in the test set is the largest. Therefore, the prediction accuracy of the RBF model is the highest, and the fitting effect is the best.

Table 2

Prediction accuracy of drag resistance for four models

Model	Training			Testing		
	R^2	RMSE	MAE	R^2	RMSE	MAE
RBF	0.9998	16.849	13.792	0.9999	9.024	5.739
BP	0.998	54.699	34.994	0.9966	79.284	63.089
DNN	0.9997	23.517	19.63	0.9986	53.814	47.1
CNN	0.9983	58.776	47.322	0.9762	201.754	138.624

Table 3

Prediction accuracy of the disturbance area of four models

Model	Training			Testing		
	R^2	RMSE	MAE	R^2	RMSE	MAE
RBF	0.9987	5.916	4.362	0.9997	2.01	1.067
BP	0.998	10.439	6.551	0.9924	13.024	12.184
DNN	0.9993	4.851	3.742	0.9968	8.702	8.118
CNN	0.9986	6.94	5.486	0.9715	24.746	22.501

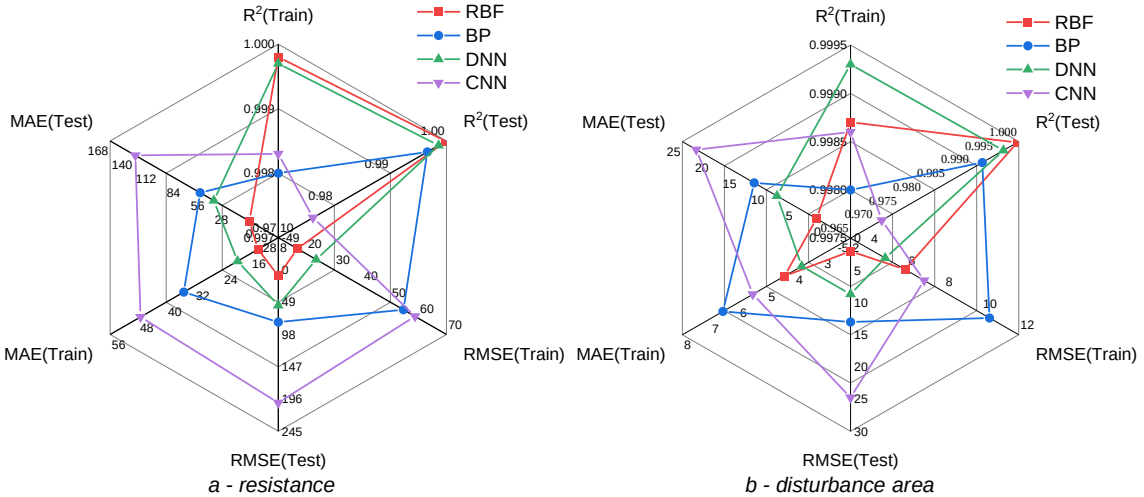

a - resistance *b - disturbance area*

Fig. 13 – Comparison of the evaluation indicators of the four models

Single output prediction results

Based on the above RBF neural network, the prediction effect is the best, and whether the accuracy of RBF neural network multi-output regression prediction is improved compared with its single output regression prediction is studied. The RBF neural network was used to predict the traction resistance and disturbance area, respectively, and the data were obtained after training, as shown in Tables 4 and 5 below. The evaluation indexes of the RBF single-output model in the test set were compared with those of the RBF multi-output model, as shown in the figure below, where R and DA are shorthand for resistance and disturbance area, respectively.

Table 4

Prediction accuracy of traction resistance of the RBF neural network

Model	Training			Testing		
	R^2	RMSE	MAE	R^2	RMSE	MAE
RBF	0.9998	16.73	13.711	0.9999	9.246	6.025

Table 5

Prediction accuracy of the disturbance area of the RBF neural network

Model	Training			Testing		
	R^2	RMSE	MAE	R^2	RMSE	MAE
RBF	0.9987	5.908	4.355	0.9997	2.01	1.107

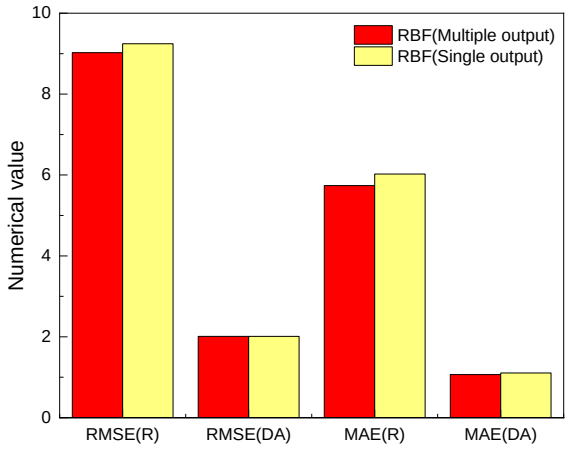

Fig. 14 - Comparison of evaluation indexes of the multi-output RBF model and the single-output RBF model

Referring to the Pearson algorithm used in Li's paper (*Li et al., 2023*) to conduct correlation analysis on velocity, depth, pressure, bulk density, water content, and resistance, this study added disturbance area on this basis to explore the correlation between resistance and disturbance area. As can be seen from the figure below, there is a strong correlation between volume weight and resistance. There is a strong correlation between water content and disturbance area.

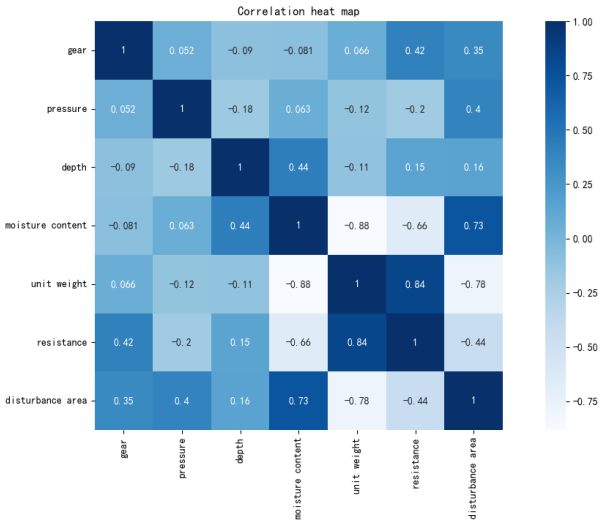

Fig. 15 - Correlation diagram

CONCLUSIONS

In this study, four neural network models (RBF, BP, DNN, and CNN) were used to make regression predictions of traction resistance and disturbance area of pneumatic subsoiling machines under the same test site in autumn and winter with inputs of subsoiling depth, velocity, pressure value, bulk density, and water content, and R^2, RMSE, and MAE as evaluation indexes. The prediction results show that the RBF model has the highest prediction accuracy, and the R^2, RMSE, and MAE of the traction resistance in the test set are 0.9999, 9.024, and 5.739, respectively, and the disturbance area is 0.9997, 2.01, and 1.067. Compared with the single output model of RBF, the MAE of the double output model of RBF is slightly lower in terms of drag resistance and disturbance area. The results show that the RBF multi-output model has a better prediction effect. Pearson correlation analysis also proves that there is a negative correlation between drag resistance and disturbance area in the process of pneumatic subsoiling. This correlation can be used to improve the accuracy of regression prediction and provide technical support for intelligent research on pneumatic subsoiling.

ACKNOWLEDGEMENT

This research was funded by the National Natural Science Foundation of China (grant nos.32171902, 32060417).

REFERENCES

[1] Aday, S.H., & Ramadhan, M.N. (2019). Comparison between the draft force requirements and the disturbed area of a single tine, parallel double tines and partially swerved double tines subsoilers. *Soil & Tillage Research*, 191, 238-244. https://doi.org/10.1016/j.still.2019.02.011

[2] Askari M., Shahgholi G., & Abbaspour-Gilandeh Y. (2017). The effect of tine, wing, operating depth and speed on the draft requirement of subsoil tillage tines. *Research in Agricultural Engineering*, 63(4), 160-167. http://dx.doi.org/10.17221/4/2016-RAE

[3] Dong, X.Q., Zheng, H.N., Chen, S., Li, Y.L., Song, J.N., & Wang, J.C. (2022). Test and analysis of vibration characteristics of vibration subsoiler. *INMATEH-Agricultural Engineering*, 68(3), 906-917. https://doi.org/10.35633/inmateh-68-90

[4] Feng, Z.Z., Li, X., Wang, W.X., Yan, Y.M., & Chen, F.X. (2019). Simulation test of pneumatic subsoiling based on pressure splitting method (基于气压劈裂法的气动深松模拟试验). *Agricultural mechanization research*, 41(11),178-184. https://link.cnki.net/doi/10.13427/j.cnki.njyi.2019.11.031

[5] Gao, A.F. (2022). *Research on tillage depth prediction model based on improved random forest* (*基于改进随机森林的耕深预测模型研究*)(Master's Degree Thesis, Changchun University of Technology).

[6] Iman, A. (2017). Effect of soil, machine, and working state parameters on the required draft force of a subsoiler using a theoretical draft-calculating model. *Soil Research*, 55(4), 389-400. https://doi.org/10.1071/SR16193

[7] Kou, L.Y. (2022). *Climate data prediction based on improved RBF neural network* (*基于改进 RBF 神经网络的气候数据预测研究*)(Msc Thesis. Southwest University of Science and Technology).

[8] Li, X., Jiang, Z.J., Wang, S.C., Li, X.L., Liu, Y., & Wang, X.H. (2023). A study of a model for predicting pneumatic subsoiling resistance based on machine learning techniques. *Agronomy*,13,1079. https://doi.org/10.3390/agronomy13041079

[9] Li, X., Wang, S.C., Meng, H.W, Qu, Q.J., & Jia, Y.W. (2022), Research on drag reduction mechanism of pneumatic subsoiler and establishment of resistance mathematical model. *Canadian Journal of Soil Science*, 102(2), 531-548. http://dx.doi.org/10.1139/cjss-2021-0101

[10] Lou, S.Y., He, J., Li, H.W., Wang, Q.J., Lu, C.Y., Liu, W.Z., Liu, P., Zhang, Z.G., & Li, H. (2021). Current knowledge and future directions for improving subsoiling quality and reducing energy consumption in conservation fields. *Agriculture*, 11, 575. https:// doi.org/10.3390/agriculture11070575

[11] Melagraki, G., Afantitis, A., Makridima, K., Sarimveis, H., & Lgglessi-Markopoulou, O. (2006). Prediction of toxicity using a novel RBF neural network training methodology. *Journal of Molecular Modeling*, 12, 297-305. https://doi.org/10.1007/s00894-005-0032-8

[12] Odey, S.O., & Manuwa, S.I. (2018). Subsoiler development trend in the alleviation of soil compaction for sustainable agricultural production. *International Journal of Engineering Inventions*, 7(8), 29-38. https://www.researchgate.net/publication/329972623

[13] Qian, J.G., Xu, W., Mu, L.L., & Wu, A.H. (2021). Calibration of soil parameters based on intelligent algorithm using efficient sampling method. *Underground Space*, 6(3), 329-341. https://doi.org/10.1016/j.undsp.2020.04.002

[14] Shi, Z.M., Chen, T.H., Li, S.T., Yang, L., & Yang, M.J. (2021). Impact of vibration on tillage performance of subsoilers using the discrete element method (DEM). *INMATEH-Agricultural Engineering*, 64(2), 89-98. https://doi.org/10.35633/inmateh-64-08

[15] Song, W.J., Choi, S.G., & Lee, E.S. (2019). Prediction and comparison of electrochemical machining on shape memory alloy(SMA) using deep neural network(DNN). *Journal of Electrochemical Science and Technology*, 10(3), 276-283. https://doi.org/10.33961/jecst.2019.03174

[16] Su, H.J., Cui, H.M., Li, F.Y., Chaolun Yideer., Zhu, Y.X., & Ma, Z.P. (2022). Vibration characteristics analysis and structure optimization of air-pressure subsoiler. *Noise & Vibration Worldwide*, 53(1-2), 12-23. https://doi.org/10.1177/09574565211052695

[17] Su, H.J., Cui, H.M., Li, F.Y., & Fan, T. (2021). Optimization design of an air-pressure subsoiler type. *INMATEH-Agricultural Engineering*, 63(1), 145-154. https://doi.org/10.35633/inmateh-63-15

[18] Tang, Z.X. (2018). *Research and implementation of air quality prediction based on BP neural network* (*基于 BP 神经网络的空气质量预测研究与实现*)(Master's Degree Thesis, Xidian University).

[19] Thomas, K., Maria, S., Tino, C., Rainer, H., & Dani, O. (2019). Historical increase in agricultural machinery weights enhanced soil stress levels and adversely affected soil functioning. *Soil & Tillage Research*, 194, 104293. https://doi.org/10.1016/j.still.2019.104293

[20] Wang, Z.Q. (2014). *Establishment of NOx emission prediction model of GA-BP diesel engine and its application on real ship* (*GA－BP 柴油机 NOx 排放预测模型的建立及实船应用研究*)(Master's Degree Thesis，Dalian Maritime University).

[21] Zhang, M.X. (2022). *Design and test of hot air deep soil opening tank test bed*(*热风式深松土槽试验台的设计与试验*). (Master's Degree Thesis，Anhui Agricultural University).

[22] Zuo, S.J. (2016), *Experimental study on the characteristics and techniques of pneumatic subsoiling* (*气压深松特性及技术的试验研究*)(Ph.D. Thesis，Northeast Agricultural University).

[23] Zuo, S.J., Kong, D.G., Chen, H.X., Han, Y., Zhang, Y., & Liu, C.S. (2017), Design of pneumatic subsoiling machine based on pressure splitting principle(基于气压劈裂原理的气压深松机设计). *Chinese Journal of Agricultural Mechanization*, 38(4), 5-10.

[24] Zuo, S.J., Kong, D.G., Liu, C.S., Li, Z.H., Zhang, C, Chen, S., & Wu, Y.F. (2017). Test and analysis of soil porosity with pneumatic subsoiling(气压深松土壤孔隙度测试与分析). *Transactions of the Chinese Society of Agricultural Engineering (Transactions of the CSAE)*, 33(1), 162-166.